# Underpotential Deposition of Metals from Thermodynamic and Structural Considerations. 2. Nonaqueous Solvents

**V. Sudha and M. V. Sangaranarayanan***

*Department of Chemistry, Indian Institute of Technology—Madras, Madras—600 036, India*

*Received: December 24, 2002; In Final Form: February 3, 2003*

The underpotential deposition (UPD) shifts of different metallic couples in acetonitrile and propylene carbonate are estimated using work function differences, lattice coordination numbers, and adsorption energies of solvent dipoles. The bulk deposition arising from monolayer and multilayer formation is considered. A satisfactory agreement of the UPD shift with the experimental data deduced from anodic stripping voltammetry is noticed. Apart from evaluating the surface potential of electrons in metals using the potential of monolayer adsorption and bulk deposition, the significance of the methodology in the development of electrochemical capacitors is indicated.

## 1. Introduction

The phenomenon of the underpotential deposition (UPD) refers to the deposition of metal adatoms on foreign substrates at potentials positive to the reversible Nernst potential. Ever since the earliest observation of UPD in systems such as Cu on Au, Tl on Ag, etc. from the characteristic (stripping) peaks in the voltammogram, the elucidation of its mechanism has remained elusive insofar as the process is dependent upon the nature of the substrate and depositing metal, adsorbed ions, and solvent molecules. However, the work function difference between the substrate and depositing species has been recognized as a predominant factor in influencing the magnitude of the UPD shift.[1,2] Subsequent investigations have focused upon the specificity of adsorption of ions, role of the single crystal and polycrystalline nature of the metallic substrate,[3−6] etc. manifested by a variety of spectroscopic observations.[7,8] In a complementary manner, the theoretical analysis of UPD has been concerned with different thermodynamic approaches[9] as well as microscopic models based on equilibrium and nonequilibrium Ising models coupled with Monte Carlo simulation procedures.[10]

In an earlier analysis[11] (hereafter referred as part 1), the UPD shifts pertaining to a variety of systems in aqueous solvents have been estimated using macroscopic thermodynamic considerations in conjunction with structural behavior of ions and solvent molecules. Since the orientational behavior of each nonaqueous solvent at electrode surfaces is different, the analysis of UPD in these systems is more involved. In this communication, we estimate the UPD shifts of a few redox couples in nonaqueous solvents, taking into account the interfacial arrangement of solvent molecules during the monolayer formation as well as bulk deposition. We also indicate a methodology by which the surface potential of electrons in metals can be deduced from the potentials of monolayer formation and bulk deposition. The usefulness of this procedure in evaluating the capacitance of UPD based supercapacitors is also indicated.

## 2. Underpotential Deposition in Nonaqueous Solvents

The parameters required for evaluating the UPD shift in aqueous solvents are as follows: (i) lattice coordination numbers, work functions of the depositing species and substrates; (ii) desorption energetics of solvent dipoles from the metal and the substrate; and (iii) adsorbate coverages, bonding behavior of the depositing species with the substrate, and partial charge transfer characteristics (cf. part 1). The UPD shift was then expressed as the difference between the potential of monolayer formation and bulk deposition. In the present analysis, the essential feature consists of the incorporation of structural details regarding the orientational behavior of nonaqueous solvent molecules. Equations 20 and 33 of part 1 yield

$$E_{ML} = -\chi_e^S - \frac{\Delta G_{desol}}{nFS_N} + \frac{\Phi_S}{CN_S} + E^\circ - \frac{\theta \Delta H_S^{desor}}{nF} - \frac{\theta \Delta H_{S-M}}{nF(CN_S)} \quad (1)$$

and

$$E_B = -\chi_e^S - \frac{\Delta G_{desol}}{nFS_N} + \frac{(1-\theta)\Phi_S}{CN_S} + \frac{\theta \Phi_M}{CN_M} + E^\circ - \frac{(1-\theta)\Delta H_S^{desor}}{nF} - \frac{(1-\theta)\Delta H_{S-M}}{nF(CN_S)} - \frac{\theta \Delta H_M^{desor}}{nF} - \frac{\theta \Delta H_{M-M}}{nF(CN_M)} \quad (2)$$

Thus, the UPD shift becomes[12]

$$\Delta E_{upd} = \theta\left(\frac{\Phi_S}{CN_S} - \frac{\Phi_M}{CN_M}\right) + (1-2\theta)\frac{\Delta H_S^{desor}}{nF} + (1-2\theta)\frac{\Delta H_{S-M}}{nF(CN_S)} + \frac{\theta \Delta H_M^{desor}}{nF} + \frac{\theta \Delta H_{M-M}}{nF(CN_M)} \quad (3)$$

In the preceding equations, the analysis pertaining to nonaqueous solvents leads to a change in their desorption energies from the substrate ($\Delta H_S^{desor}$) and depositing species ($\Delta H_M^{desor}$); the work functions of the substrate and depositing species are denoted as $\Phi_S$ and $\Phi_M$, respectively, $CN_S$ and $CN_M$ being the coordination numbers. $\Delta H_{S-M}$ and $\Delta H_{M-M}$ indicate the enthalpy change in the formation of substrate−metal and metal−metal bonds, respectively. The number of electrons transferred is denoted by $n$. Further, whenever a partial charge transfer occurs

10.1021/jp027818m CCC: $25.00 
Published on Web 03/28/2003

between the substrate and adsorbate, it is essential to introduce the charge on the adsorbate ($z_{ad}$) in lieu of $n$. Equation 3 is valid if a complete monolayer is formed during the bulk deposition. In the case of UPD in aqueous solvents, the values of $z_{ad}$ are, in general, nonintegers.[2] In a fortuitous manner, for nonaqueous solvents, when the depositing species are alkali metals, $n = z_{ad}$ is shown to be unity,[13] indicating a complete discharge of the ions. This feature provides considerable simplicity in the analysis.

**2.1. Adsorption Behavior of Nonaqueous Solvents at Electrodes.** The orientational states of nonaqueous solvents on the substrate as well as the depositing metal are different; hence, their interaction energies with the electrode surfaces and metal adatoms need to be incorporated, and an approximate method for estimating $\Delta H_S^{desor}$ and $\Delta H_M^{desor}$ is proposed here. Among various nonaqueous solvents, acetonitrile (ACN) and propylene carbonate (PC) are widely employed, the depositing species in general being alkali metals. Hence, the UPD shift pertaining to the alkali metals in the above solvents is analyzed for different electrodes.

*(i) Acetonitrile (ACN).* The orientation of ACN at Pt electrodes has been deduced using potentiodynamic studies which indicate that the bonding of ACN with the metal will be via the nitrile group;[14] however, it may be either through the carbon or nitrogen atom of the nitrile group. From the surface enhanced Raman scattering (SERS) investigations of Pt in ACN,[15] it has been reported that the potential of zero charge of Pt is shifted to more negative values[16] implying the involvement of nitrogen atoms in bonding with the metal surface. This is interpreted in terms of the electrochemical Stark effect, wherein electrons from Pt are donated to the $5\sigma$ antibonding orbital of $CN^-$ group.[17] Further, in the case of alkali metals such as $Li^+$, too, from the stretching frequency of CN in SERS studies, it is deduced that the adsorption of ACN will be via the nitrogen atom.[18] In the presence of $LiClO_4$ in ACN,[19] $ClO_4^-$ ions will preferentially adsorb through the carbon atom of the CN group while $Li^+$ will bond via the nitrogen atom of CN. Hence, the N-atom of the CN group is involved in the adsorption of ACN on noble metals as well as alkali metals[18,20] viz. $H_3C{-}C{\equiv}N{\cdots}Pt$ for Pt as the substrate and $H_3C{-}C{\equiv}N{\cdots}Li^+$ for underpotentially depositing species such as Li. Thus, the enthalpy of desorption of ACN can be written as

$$\Delta H_S^{desor} \approx \Delta H_{S-N} \quad \text{and} \quad \Delta H_M^{desor} \approx \Delta H_{M-N}$$

where $\Delta H_{S-N}^{desor}$ and $\Delta H_{M-N}^{desor}$ represent the enthalpies of dissociation of substrate−nitrogen and metal−nitrogen bonds, available in tabular compilations[21] for a few selected systems. It may also be estimated in an approximate manner from Pauling's arithmetic mean[22] formula viz.

$$DE_{A-B} = \frac{1}{2}[DE_{A-A} + DE_{B-B}] + 23.06[x_A - x_B]^2 \quad (4)$$

wherever necessary. In eq 4, A may denote either the substrate or the depositing species as the case may be while B indicates here the nitrogen atom. $DE_{A-B}$ is the dissociation energy of the substrate−nitrogen or metal−nitrogen bond; $DE_{A-A}$ represents the dissociation energies of the substrate−substrate or metal−metal bond and $DE_{B-B}$ that of the nitrogen−nitrogen bond. $\chi_A$ and $\chi_B$ denote the Pauling electronegativities of the substrate or depositing species and nitrogen atoms, respectively. Thus, eq 4 enables the calculation of S−N and M−N dissociation enthalpies from those due to S−S, M−M, and N−N bonds and appropriate electronegativities in the Pauling scale. The values of $\Delta H_{S-N}$ and $\Delta H_{M-N}$ for the chosen UPD systems are provided in section 2.2.2.

*(ii) Propylene Carbonate (PC).* From the vibrational stretching bands observed in Fourier transform infrared (FTIR) studies, it has been deduced that PC will bond through the oxygen atom in the case of alkali metals[23,24] as well as noble metals.[25] It is further supported from FTIR spectroscopy, wherein the cleavage of PC in Li salts into lithium alkyl carbonates occurs when the potential is increased.[25] Thus, the orientation of PC may be denoted as[23]

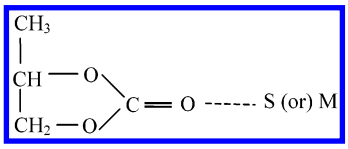


leading to the enthalpy of desorption of solvent dipoles from substrate and depositing species as

$$\Delta H_S^{desor} \approx \Delta H_{S-O} \quad \text{and} \quad \Delta H_M^{desor} \approx \Delta H_{M-O}$$

where $\Delta H_{S-O}$ and $\Delta H_{M-O}$ represent the substrate−oxygen and metal−oxygen bond dissociation enthalpies. The estimates of $\Delta H_{S-O}$ and $\Delta H_{M-O}$ for various UPD systems ($S/M^{n+}$) in PC are discussed in section 2.2.2.

**2.2. Parameters Employed in the Estimation of UPD Shift.** Although the UPD shifts for a large number of redox systems in nonaqueous solvents have been studied till now, the calculation is restricted here to those couples for which all the required parameters are available from experimental data. Consequently, the UPD shifts of five systems viz. Au/$Li^+$(ACN), Cu/$Li^+$(PC), Pt/$Li^+$(PC), Pt/$Na^+$(PC), and Pt/$Cs^+$(PC) are considered here.

*2.2.1. Estimation of Surface Coverages.* The estimation of the surface coverages plays a crucial role in UPD phenomena, and in principle, the surface coverages are influenced by the surface topography, extent of roughness, pretreatment procedures, etc. Hence, a first-principles evaluation of the same is rendered difficult. To circumvent this limitation, it is judicious to employ experimental data such as charges deduced from the cyclic voltammetry in conjunction with an assumed adsorption isotherm. However, the appearance of the well-defined peaks in the cyclic voltammogram is essential to employ this strategy. For example, the UPD studies of Cd and Te on polycrystalline Au, Pt, and Cu substrates investigated using thin layer electrochemical cells in aqueous solvents exhibit cyclic voltammetry peaks which are not sharp.[26] Further, ill-defined peaks[27] are noticed in the UPD of Cd on Ag(111) from propylene carbonate solutions as well as in the self-assembled monolayer studies of metallophthalocyanine complexes pertaining to UPD of Cu on Au electrodes.[28] Consequently, the estimation of the surface coverage from the half-width potential is not possible in such cases. An alternate methodology would be to employ optimization procedures to obtain the best set of parameters for charge densities and surface coverages from adsorption isotherms.

In UPD systems exhibiting well-defined peaks, the Frumkin isotherm (FI) may be employed on account of the simple manner in which the half-width potential $\Delta V_{1/2}$ is related to the interaction constant $a$ as[29]

$$\Delta V_{1/2} = \frac{2RT}{F}\ln\left[\frac{(a+4)^{1/2} + (a+1)^{1/2}}{(a+4)^{1/2} - (a+1)^{1/2}}\right] + \frac{2aRT}{nF}\left[\frac{(a+1)}{(a+4)}\right]^{1/2} \quad (5)$$

By solving the preceding equation using the experimental half-

**TABLE 1: Determination of the Surface Coverage of the Depositing Species from the Peak Current and Corresponding Charge Densities**

| system S/M$^{n+}$ | $\Delta V_{1/2}$[a] | $a$[b] | $i_p$[c] | $q_p$[d] | $\theta$ ($q_p/q_{max}$)[e] |
|---|---|---|---|---|---|
| Au/Li$^+$ (ACN) | 0.53 | 7.94 | 140.00[f] | 714.75 | 0.62 |
| Cu/Li$^+$ (PC) | 0.35 | 4.67 | 110.00[f] | 376.75 | 0.33 |
| Pt/Li$^+$ (PC) | 0.50 | 7.37 | 111.67[51] | 538.54 | 0.57 |
| Pt/Na$^+$(PC) | 0.27 | 3.23 | 53.33[51] | 143.20 | 0.38 |
| Pt/Cs$^+$ (PC) | 0.26 | 3.05 | 16.67[51] | 43.21 | 0.36 |

[a] Experimental[2] half-width potential (V). [b] Frumkin interaction constant calculated using eq 5. The values of $a$ are obtained from eq 5 using MATLAB 6.0 version. [c] Peak current density ($\mu$A cm$^{-2}$). [d] Charge due to the adsorbed species ($\mu$C cm$^{-2}$) using eq 6. [e] Surface coverage. [f] The peak current densities are estimated from the corresponding experimental cyclic voltammetric peaks.[1]

potential widths, the values of $a$ are obtained (Table 1), and the positive values of $a$ represent the repulsive interaction between the adsorbate species.[29] Subsequently, $q_p$ is estimated from[30]

$$q_p = \frac{i_p RT(2a + 4)}{nFA\nu} \tag{6}$$

where $i_p$ denotes the peak current density, $\nu$ is the scan rate, and $q_p$ is the charge deduced from $i_p$ (cf. Scheme 1). $n$ represents the number of electrons transferred, and in the case of a partial charge transfer, $n = z_{ad}$. As mentioned earlier, with $z_{ad}$ being unity in the case of alkali metals, eq 6 enables the estimation of $q_p$. Further, the surface coverage $\theta$ is given as $q_p/q_{max}$ where $q_{max}$ denotes the charge density associated with maximum surface excess obtainable from geometrical considerations using the expression[31]

$$q_{max} = |z|e/d_a^2 \tag{7}$$

where $z$ is the charge of the depositing species, $e$ is the electronic charge, and $d_a$ denotes the diameter of the adsorbate. The values of $q_{max}$ pertaining to $Li^+$, $Na^+$, and $Cs^+$ are estimated to be 1150.53, 408.63, and 143.61 $\mu$C cm$^{-2}$ using the corresponding ionic diameters[21] 1.18, 1.98, and 3.34 Å. The surface coverages

**TABLE 2: Enthalpy Change Associated with the Desorption of Solvent Molecules from the Substrate (S) and Underpotentially Deposited Metals (M)**

| UPD system S/M$^{n+}$ | nonaqueous solvent | $\Delta H_S^{desor}$ (kJ mol$^{-1}$) | $\Delta H_M^{desor}$ (kJ mol$^{-1}$) |
|---|---|---|---|
| Au/Li$^+$ | acetonitrile (ACN) | 594.07[a] | 620.01[a] |
| Cu/Li$^+$ | propylene carbonate (PC) | 269.00[b] | 333.50[b] |
| Pt/Li$^+$ | propylene carbonate (PC) | 391.60[b] | 333.50[b] |
| Pt/Na$^+$ | propylene carbonate (PC) | 391.60[b] | 256.10[b] |
| Pt/Cs$^+$ | propylene carbonate (PC) | 391.60[b] | 295.80[b] |

[a] The estimates of $\Delta H_S^{desor}$ and $\Delta H_M^{desor}$ are obtained using eq 4. [b] The values of $\Delta H_{S-O}$ and $\Delta H_{M-O}$ are from Lide.[21]

pertaining to the UPD systems using eqs 6 and 7 are reported in Table 1. In order to verify the validity of this procedure, $q_p$ for the system Au/Li$^+$(ACN) was deduced from eq 6 as well as integration of the corresponding cyclic voltammetric peak,[32] and the values differ by ca. 4%.

*2.2.2. Evaluation of $\Delta H_S^{desor}$ and $\Delta H_M^{desor}$ for the UPD Systems.* The parameters $\Delta H_S^{desor}$ and $\Delta H_M^{desor}$ for the systems Au/Li$^+$(ACN), Cu/Li$^+$(PC), Pt/Li$^+$(PC), Pt/Na$^+$(PC), and Pt/Cs$^+$(PC) are evaluated as follows: in the case of Au/Li$^+$ in ACN, $\Delta H_S^{desor} \approx \Delta H_{S-N}$ and is estimated from Pauling's arithmetic mean formula (eq 4) using the values of $DE_{Au-Au}$,[21] $DE_{N-N}$,[21] $\chi_{Au}$,[22] and $\chi_N$[22] as 226.20 kJ mol$^{-1}$, 945.33 kJ mol$^{-1}$, 2.4, and 3.0, respectively. Similarly, eq 4 is employed to obtain $\Delta H_M^{desor}$ vis-á-vis $\Delta H_{M-N}$; the values[21] of $DE_{Li-Li}$ and $DE_{N-N}$ are 110.21 kJ mol$^{-1}$ and 945.33 kJ mol$^{-1}$, respectively, while the Pauling electronegativities[23] of Li and N are 1.0 and 3.0. For other systems Cu/Li$^+$, Pt/Li$^+$, Pt/Na$^+$, and Pt/Cs$^+$ in PC, $\Delta H_S^{desor}$ is assumed as $\Delta H_{S-O}$ (S being Cu and Pt) and $\Delta H_M^{desor}$ as $\Delta H_{M-O}$ where M is Li, Na, or Cs (cf. section 2.1) whose estimates are available in tabular compilations[21] (Table 2).

*2.2.3 Coordination Numbers of the Substrate and Depositing Species.* The coordination number of the substrate ($CN_S$) and that of the depositing species ($CN_M$) appear in the expression for the UPD shift. In the case of the depositing species, $CN_M$ may be taken as the lattice coordination number, whereas for the substrates, the value of $CN_S$ indicates their ability to form

**SCHEME 1: Methodology for Estimating the UPD Shift in Nonaqueous Solvents**

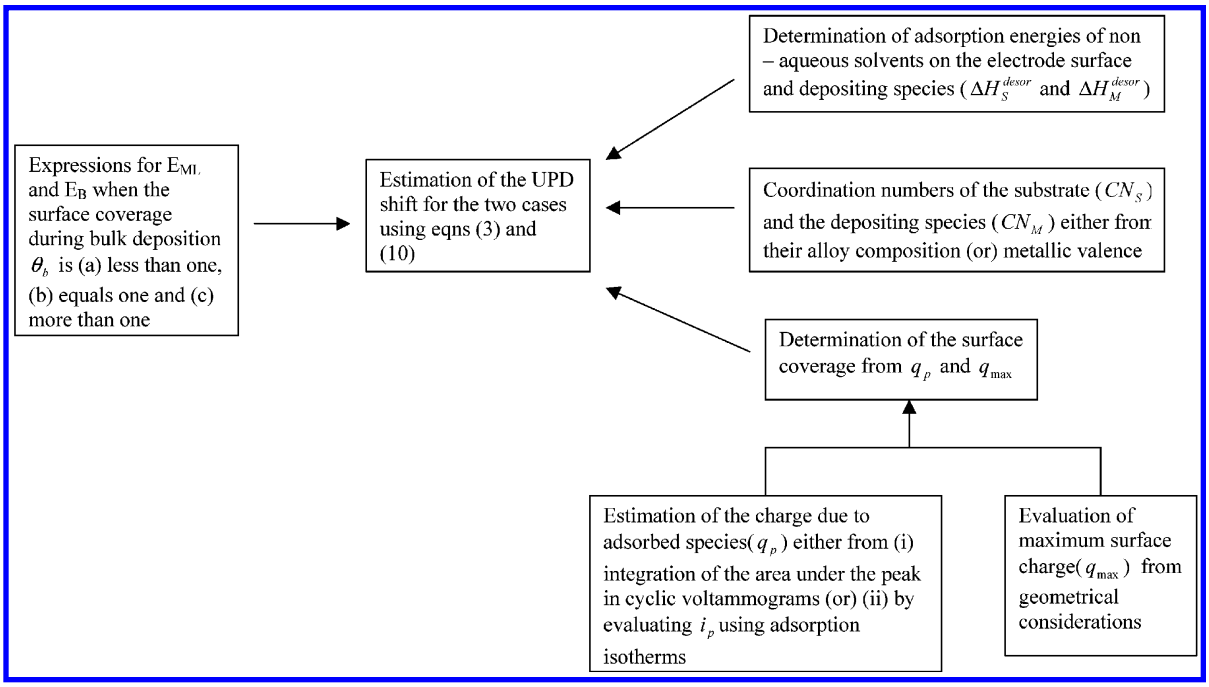

**TABLE 3: Parameters Employed in Estimating the UPD Shift Using Equation 3**[a]

| system S/M$^{n+}$ | nonaqueous solvent | $\Phi_S$ (eV)[40] | $\Phi_M$ (eV)[40] | $CN_S$ | $\Delta H_{S-M}$ (kJ mol$^{-1}$) | $\Delta H_{M-M}$ (kJ mol$^{-1}$)[21] | $\Delta E_{upd}^{expt}$ [c] | $\Delta E_{upd}^{cald}$ [d] |
|---|---|---|---|---|---|---|---|---|
| Au/Li$^+$ | ACN | 4.80 | 3.1 | 2.82[35] | −284.50[21] | −110.21 | 1.23 | 1.18 |
| Cu/Li$^+$ | PC | 4.55 | 3.1 | 3.00[33] | −192.90[21] | −110.21 | 1.05 | 0.96 |
| Pt/Li$^+$ | PC | 5.03 | 3.1 | 1.50[35] | −241.81[b] | −110.21 | 1.56 | 1.35 |
| Pt/Na$^+$ | PC | 5.03 | 2.7 | 6.00[22] | −229.01[b] | −73.08 | 1.30 | 1.11 |
| Pt/Cs$^+$ | PC | 5.03 | 1.9 | 6.00[22] | −227.35[b] | −43.92 | 2.00 | 1.93 |

[a] The surface coverages are reported in Table 1. The coordination number of the metal adatoms $CN_M$ is unity[22] while the values of $\Delta H_S^{desor}$ and $\Delta H_M^{desor}$ are as given in Table 2. [b] $\Delta H_{S-M} = -DE_{S-M}$, and these are estimated from Pauling's arithmetic mean (eq 4) using $DE_{Pt-Pt}$[21] and $\chi_{Pt}$[22] as 307.00 kJ mol$^{-1}$ and 2.2, respectively. The values of $DE_{M-M}$ pertaining to Li−Li, Na−Na, and Cs−Cs are from column 7 of this table while $\chi_M$[22] of Li, Na, and Cs is 1.0, 0.9, and 0.7, respectively. [c] Experimental UPD shift.[1] [d] Calculated UPD shift from eq 3.

appropriate alloys and metallic valences may be taken as the characteristic parameters instead of the lattice coordination numbers.

Since our emphasis here pertains to the UPD of alkali metals from nonaqueous solvents, the formation of their alloys[2,33] with substrates needs to be considered. Thus, the lattice coordination number $CN_S$ of the substrate is replaced by its metallic valence, which is deduced from the composition of the alloys. Li forms an alloy[34] with Cu which has the composition $Li_3Cu$. Hence, for the UPD couple Cu/Li$^+$ (from PC), $CN_S$ equals 3. Analogously, when the substrates are Au and Pt, the corresponding alloys have the composition[35] $Li_{2.82}Au$ and $Li_3Pt_2$. Consequently, in the UPD systems Au/Li$^+$(ACN) and Pt/Li$^+$(PC), the coordination number of Au and Pt equals 2.82 and 1.5, respectively. However, since Pt does not form alloys with Na and Cs, its $CN_S$ equals 6 which is the metallic valence[22] of Pt. The coordination numbers of the depositing species ($CN_M$'s) are considered as their corresponding metallic valence and equal unity for the alkali metals.[22]

*2.2.4. Estimation of the UPD Shift.* For the UPD systems in aqueous solvents (part I), the charge densities associated with the partial charge transfer ($z_{ad}$) were ferreted out from various experimental data, viz. in the case of systems such as Ag/Tl$^+$, Pt/Cu$^{2+}$, and Au/Pb$^{2+}$ in aqueous electrolytes, a partial charge transfer occurs, and hence, the values of $n$ have been deduced[36,37] as 3.53, 1.0, and 1.5, respectively. In contrast, for nonaqueous solvents, $z_{ad}$ is nearly unity indicating a complete discharge of alkali ions. However, only when such a simplification exists and well-defined UPD peaks are observed, the methodology advocated herein becomes applicable.

Equation 3 enables the computation of the UPD shift for various couples with the help of (i) energetics concerning the interfacial solvent structure, (ii) molecular and geometrical parameters pertaining to the depositing species and substrate, and (iii) surface coverages deduced from the half-potential width data (cf. Scheme 1). In Table 3, the calculated UPD shifts for various couples in ACN and PC have been reported, and $n$ is assumed to be unity since the reduction of alkali metals has been shown to undergo a complete one-electron transfer.[13] While the agreement with the experimentally obtained UPD shift is satisfactory, it may be pointed out that the bond dissociation energies, adsorbate sizes, and coordination numbers are somewhat approximate estimates. Nevertheless, it is gratifying to note that the quantitative influence of each system parameter appears in the expression for the UPD shift.

**2.3. Estimation of the UPD Shift When Less Than One Monolayer Is Formed During the Bulk Deposition.** The expression for the potential of bulk deposition (section 2) is valid if a complete monolayer is formed during the bulk deposition which is composed of (i) the deposition of metal adatoms on the vacant sites $(1-\theta)$ of the substrate and (ii) the deposition on the underpotentially deposited sites ($\theta$) of the metal adatoms. If the surface coverage of metal adatoms during the bulk deposition is less than unity, two different surface coverages viz. $\theta_{ML}$ and $\theta_b$ arise where $\theta_{ML}$ is the surface coverage of the metal adatoms during the monolayer formation and $\theta_b$ denotes the same during the bulk deposition (Scheme 2). The sum of these two coverages yields $\theta_t$ ($\theta_{ML} + \theta_b = \theta_t$) where $\theta_t$ represents the total surface coverage of the process. Further, $\theta_b$ itself consists of (a) the deposition of metal adatoms on the vacant $(1-\theta_{ML})$ sites of the substrate (S) and (b) the deposition of M on $(\theta_t - 1)$ sites of the underpotentially deposited metal adatoms. Thus, the sum of $(1-\theta_{ML})$ and $(\theta_t - 1)$ equals the bulk deposition coverage, $\theta_b$. Hence, the expression for $E_{ML}$ becomes

$$E_{ML} = -\chi_e^S - \frac{\Delta G_{desol}}{nFS_N} + \frac{\Phi_S}{CN_S} + E^\circ - \frac{\theta_{ML}\Delta H_{desor}^S}{nF} - \frac{\theta_{ML}\Delta H_{S-M}}{nF(CN_S)} \quad (8)$$

by substituting $\theta_{ML}$ instead of $\theta$ in eq 1. Similarly, $E_B$ is given by

$$E_B = -\chi_e^S - \frac{\Delta G_{desol}}{nFS_N} + \frac{(1-\theta_{ML})\Phi_S}{CN_S} + \frac{(\theta_t - 1)\Phi_M}{CN_M} + E^\circ - \frac{(1-\theta_{ML})\Delta H_S^{desor}}{nF} - \frac{(1-\theta_{ML})\Delta H_{S-M}}{nF(CN_S)} - \frac{(\theta_t - 1)\Delta H_M^{desor}}{nF} - \frac{(\theta_t - 1)\Delta H_{M-M}}{nF(CN_M)} \quad (9)$$

by substituting $(1-\theta_{ML})$ and $(\theta_t - 1)$ instead of $(1-\theta)$ and $\theta$, respectively, in eq 2.

The UPD shift ($\Delta E_{upd}$) resulting from the above eqns is

$$\Delta E_{upd} = \theta_{ML}\frac{\Phi_S}{CN_S} - (\theta_t - 1)\frac{\Phi_M}{CN_M} + (1-2\theta_{ML})\frac{\Delta H_S^{desor}}{nF} + (1-2\theta_{ML})\frac{\Delta H_{S-M}}{nF(CN_S)} + (\theta_t - 1)\frac{\Delta H_M^{desor}}{nF} + (\theta_t - 1)\frac{\Delta H_{M-M}}{nF(CN_M)} \quad (10)$$

In the underpotential deposition of Cu$^+$ on Au in ACN, the bulk deposition involves the formation of submonolayers, and it is instructive to employ eq 10 for this system. The (sub)-monolayer coverage $\theta_{ML}$ and the bulk deposition coverage ($\theta_b$) are reported as 0.65 and 0.55, respectively, from their corresponding stripping peaks,[38] and hence, the total coverage ($\theta_t$) leads to 1.2 monolayers (MLs). The parameters employed for the estimation of $\Delta E_{upd}$ are as follows: the work functions of Au and Cu, the enthalpy of desorption of solvent dipoles from

**SCHEME 2: Representation of the UPD and Bulk Deposition Process When (a) Less than One Monolayer, (b) One Monolayer, and (c) More than One Monolayer Is Formed**

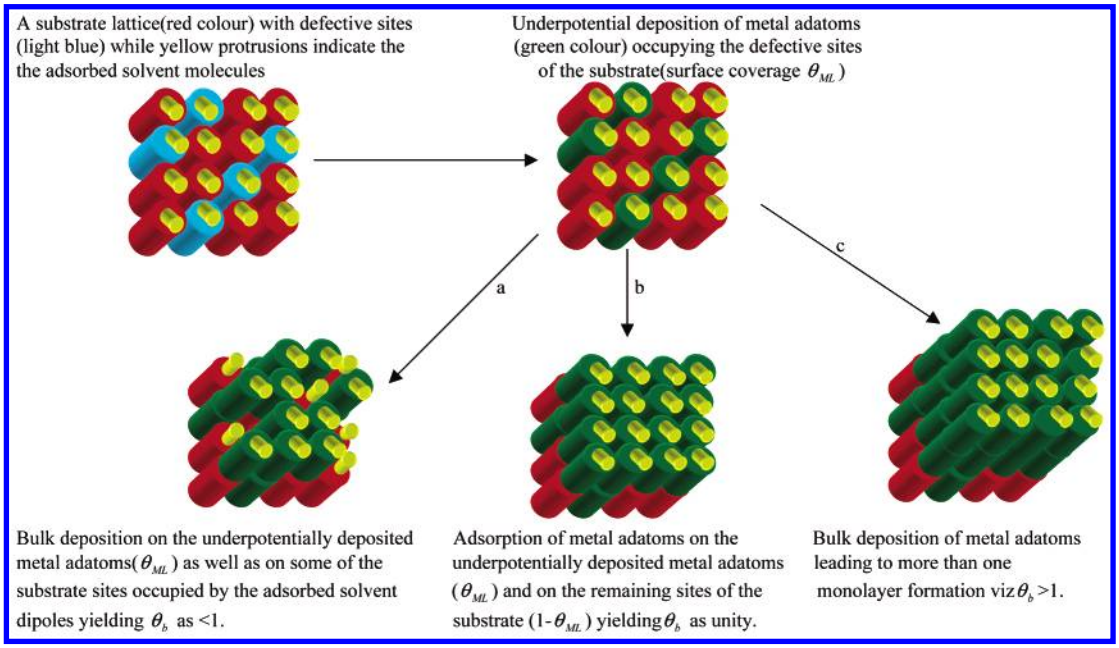


Au, and the coordination numbers of Au and Cu are as mentioned earlier; the enthalpy of desorption of solvent dipoles from Cu is evaluated from eq 4 as 588.83 kJ mol$^{-1}$ by substituting the values of $DE_{Cu-Cu}$,[21] $DE_{N-N}$,[21] $\chi_{Cu}$,[22] and $\chi_N$[22] as 176.52 kJ mol$^{-1}$, 945.33 kJ mol$^{-1}$, 1.9, and 3, respectively. The enthalpies of formation of Au−Cu and Cu−Cu bonds are available in tabular compilations[21] as −228.00 and −176.52 kJ mol$^{-1}$, respectively, while the number of electrons transferred is assumed to be unity in the reduction of $Cu^+$ to Cu on account of the complete one-electron transfer. Consequently, the value of $\Delta E_{upd}$ for this system deduced using eq 10 is 0.310 V which is in satisfactory agreement with the experimental value of 0.325 V deduced from the stripping peaks of UPD and overpotential deposition (OPD) in the cyclic voltammogram.[38]

### 3. Estimation of the Surface Potential of Electrons in Metals

It is instructive to enquire whether the potential of monolayer formation ($E_{ML}$) and that due to the bulk deposition ($E_B$) which yield the UPD shift may be employed to deduce other parameters of interest in chemical physics. This issue is of relevance since electrode kinetic data were shown to yield metallic hardness, hitherto obtainable only from density functional theories.[39] The surface potential of ions is a measure of the energy required for them to cross the solution−vacuum interface during their desolvation. Under electronic equilibrium,[40] the surface potential of metal ions ($\chi_{M^{n+}}$) in a chosen solvent equals $z\chi_e^{(s)}$ where $\chi_e^{(s)}$ denotes the surface potential of electrons in solution, $z$ being the charge of the metal ion. Further, $\chi_e^{(s)} = \chi_e^S$, the surface potential of electrons in the substrate (S). Since the UPD shift ($\Delta E_{upd}$) denotes the difference between $E_{ML}$ and $E_B$, the surface potentials themselves do not appear in it; however, the expressions for $E_{ML}$ and $E_B$ contain the surface potential of electrons in solution which may be exploited.

**3.1. Surface Potential of Electrons in the Substrate from the Potential of Monolayer Adsorption.** Equations 1 and 8 yield the potential of monolayer adsorption when $\theta_b = 1$ and $\theta_b < 1$, respectively. The UPD systems Cu/$Li^+$(PC) and Au/$Li^+$(ACN) are considered here for which $\theta_b$ is unity. For the system Cu/$Li^+$ in PC, $\chi_e^S$ is obtained by rearranging eq 1 as

$$\chi_e^S = -E_{ML} - \frac{\Delta G_{desol}}{nFS_N} + \frac{\Phi_S}{CN_S} + E^\circ - \frac{\theta \Delta H_S^{desor}}{nF} - \frac{\theta \Delta H_{S-M}}{nF(CN_S)} \quad (11)$$

Employing the value of $\Delta G_{desol}$ of $Li^+$ in PC as[41] 397.48 kJ mol$^{-1}$, we obtain $\chi_e^S$ as −1.61 eV for Cu in PC. However, the real desolvation energy $\Delta G_{desol}^{real}$ is defined for an ion of valency $z$ as[42]

$$\Delta G_{desol} = \Delta G_{desol}^{real} - zF\chi_e^{(s)} \quad (12)$$

and by substituting the preceding equation in eq 1, we obtain

$$\chi_e^S\left(\frac{1}{S_N} + 1\right) = -E_{ML} - \frac{\Delta G_{desol}^{real}}{nFS_N} + \frac{\Phi_S}{CN_S} + E^\circ - \frac{\theta \Delta H_S^{desor}}{nF} - \frac{\theta \Delta H_{S-M}}{nF(CN_S)} \quad (13)$$

if $n$ equals $z_{ad}$ as mentioned earlier. For $Li^+$ in ACN, $\Delta G_{desol}^{real}$ has been reported as[43] 506.68 kJ mol$^{-1}$, thus yielding the surface potential of electrons in Au from eq 13 as −2.82 eV. The large value of $\chi_e^S$ for Au in ACN may be attributed to the higher enthalpy of desorption of ACN on Au.

Analogously, for the system Au/$Cu^+$(ACN) wherein $\theta_b < 1$ and for which $\Delta G_{desol}^{real}$ is reported, we obtain

$$\chi_e^S\left(\frac{1}{S_N} + 1\right) = -E_{ML} - \frac{\Delta G_{desol}^{real}}{nFS_N} + \frac{\Phi_S}{CN_S} + E^\circ - \frac{\theta_{ML} \Delta H_S^{desor}}{nF} - \frac{\theta_{ML} \Delta H_{S-M}}{nF(CN_S)} \quad (14)$$

from eqs 8 and 12. $\chi_e^S$ for Au deduced from the preceding equation using $\Delta G_{desol}^{real}$ as[43] 644.34 kJ mol$^{-1}$ yields −2.91 eV (cf. Table 4).

**TABLE 4: Estimation of the Surface Potential of Electrons in Metals from the Potentials of Monolayer Formation and Bulk Deposition**

| system S/$M^{n+}$ | potentials (V) | surface potential of electrons in the substrate $\chi_e^S$(eV) | parameters required for computing $\chi_e^S$ |
|---|---|---|---|
| Cu/$Li^+$(PC) | $E_{ML}$ (−1.40 vs SCE)[1] | −1.61 (from eq 11) | $E°$ ($Li^+$/Li)[52] = − 3.27V; $\Delta G_{desol}$ of $Li^+$ in PC[41] = 397.48 kJ $mol^{-1}$; $S_N = 4$[53a] |
| | $E_B$ (−2.40 vs SCE)[1] | −1.58 (from eq 15) | |
| Au/$Li^+$ (ACN) | $E_{ML}$ (−1.75 vs SCE)[1] | −2.82 (from eq 13) | $E°$ ($Li^+$/Li)[52] = − 2.93 V; $\Delta G_{desol}^{real}$ of $Li^+$ in ACN[42] = 506.68 kJ $mol^{-1}$; $S_N = 8$[54] |
| | $E_B$ (−2.90 vs SCE)[1] | −2.85 (from eq 16) | |
| Au/$Cu^+$(ACN) | $E_{ML}$ (0.10 vs $Ag^+$/Ag)[38] | −2.91 (from eq 14) | $E°$ ($Cu^+$/Cu) in ACN[41] = − 0.58 V; $\Delta G_{desol}^{real}$ of $Cu^+$ in ACN[42] = 644.34 kJ $mol^{-1}$ $S_N = 8$[53b] |
| | $E_B$ (−0.225 vs $Ag^+$/Ag)[38] | −2.89 (from eq 17) | |

**3.2. From the Potential of Bulk Deposition.** For the system Cu/$Li^+$ in PC, the estimation of $\chi_e^S$ from $E_B$ (eq 2) leads to

$$\chi_e^S = -E_B - \frac{\Delta G_{desol}}{nFS_N} + \frac{(1-\theta)\Phi_S}{CN_S} + \frac{\theta\Phi_M}{CN_M} + E° - \frac{(1-\theta)\Delta H_S^{desor}}{nF} - \frac{(1-\theta)\Delta H_{S-M}}{nF(CN_S)} - \frac{\theta\Delta H_M^{desor}}{nF} - \frac{\theta\Delta H_{M-M}}{nF(CN_M)} \quad (15)$$

Employing the parameters reported in Table 4 for Cu/$Li^+$ in PC, we obtain $\chi_e^S$ as −1.58 eV. Thus, the value of $\chi_e^S$ for Cu in PC shows agreement with that of $\chi_e^S$ deduced from the expression for $E_{ML}$ (eq 11). As mentioned earlier, in the case of Au/$Li^+$ in ACN, eq 2 in conjunction with eq 12 yields

$$\chi_e^S\left(\frac{1}{S_N}+1\right) = -E_B - \frac{\Delta G_{desol}^{real}}{nFS_N} + \frac{(1-\theta)\Phi_S}{CN_S} + \frac{\theta\Phi_M}{CN_M} + E° - \frac{(1-\theta)\Delta H_S^{desor}}{nF} - \frac{(1-\theta)\Delta H_{S-M}}{nF(CN_S)} - \frac{\theta\Delta H_M^{desor}}{nF} - \frac{\theta\Delta H_{M-M}}{nF(CN_M)} \quad (16)$$

$\chi_e^S$ for Au in ACN obtained from the preceding equation using the parameters reported in Table 4 equals −2.85 eV. Analogously, for the system Au/$Cu^+$ (ACN), from eqs 9 and 12, we obtain

$$\chi_e^S\left(\frac{1}{S_N}+1\right) = -E_B - \frac{\Delta G_{desol}^{real}}{nFS_N} + \frac{(1-\theta_{ML})\Phi_S}{CN_S} + \frac{(\theta_t-1)\Phi_M}{CN_M} + E° - \frac{(1-\theta_{ML})\Delta H_S^{desor}}{nF} - \frac{(1-\theta_{ML})\Delta H_{S-M}}{nF(CN_S)} - \frac{(\theta_t-1)\Delta H_M^{desor}}{nF} - \frac{\theta_{ML}\Delta H_{M-M}}{nF(CN_M)} \quad (17)$$

Employing the parameters as indicated earlier, $\chi_e^S$ for Au in ACN is estimated from eq 17 (cf. Table 4). It is of interest to note that $\chi_e^S$ for Au obtained from the potential of monolayer formation and bulk deposition is consistent with each other.

## 4. Perspectives and Summary

The foregoing analysis has provided a phenomenological framework for evaluating the UPD shift in nonaqueous solvents by incorporating the characteristic features pertaining to the substrate and depositing species along with appropriate bonding considerations. In view of the intricate specificities concerning the UPD process in itself, a global validity of the present formalism may not be possible. While macroscopic considerations such as the one presented here are worthwhile regarding the qualitative insights they offer, a few limitations of the formalism exist. Among them, mention may be made of (i) the need to have well-defined peaks in cyclic voltammograms essential for employing eq 5, (ii) the necessity for systems wherein no predominant attractive interactions between the adsorbates exist, and (iii) the quantitative estimate of the adsorbate charge densities ($z_{ad}$) in relation to the number of electrons ($n$) involved in the discharge of the ionic species. However, on account of the importance of the UPD in the development of fuel cells,[44] supercapacitors,[45] as well as nanomaterials,[46] a macroscopic methodology is worthwhile for delineation of the processes involved, even for simple systems.

The UPD phenomenon in the presence of adsorbed ions[47,48] is an interesting study in view of the rich structural features and diverse types of phase transitions.The methodology advocated here will be invalid in such cases on account of exclusion of coadsorption of ionic species. Nevertheless, by including the competition of ionic adsorbates with solvent dipoles for lattice sites, this subtle effect may be analyzed at a coarse-grained level of description. This will then enable the mapping of qualitative thermodynamic interpretations with spectroscopic data[8] as well as diverse statistical mechanical models.[49] A recent study employing the fast Fourier transform impedance spectroscopy[50] in conjunction with potential perturbation techniques concerning the UPD of Bi in the presence of electrosorption of $ClO_4^-$ ions deserves mention in this context.

A plausible application of the present methodology consists of analyzing the influence of various thermodynamic factors governing the magnitude of pseudocapacitance ($C_\phi$) arising out of the UPD-based supercapacitors. Since the ratio between the accumulated charge and the corresponding potential dictates the capacitance, eqs 1 and 2 which incorporate different energetic contributions involving the depositing species, solvent dipoles, and the electrode substrate provide a preliminary estimate of the capacitances. The values of $C_\phi$ for couples such as Au/$Li^+$-(ACN), Cu/$Li^+$(PC), Pt/$Li^+$(PC), Pt/$Na^+$(PC), and Pt/$Cs^+$(PC), deduced using $q_p$ (from eq 6) and the potential window,[1,13] span a range ca. 40−240 $\mu$F $cm^{-2}$. However, further refinements regarding the role of adsorbate−adsorbate interactions, nature of adsorption isotherms, coupling between faradaic and nonfaradaic processes, etc. need to be carried out for obtaining more reliable estimates.

In summary, a phenomenological methodology for the analysis of the UPD shift in nonaqueous solvents is proposed, and the qualitative influence of various system parameters has been pointed out. The surface potential of electrons in metals

is deduced from the data pertaining to the potentials of monolayer formation and bulk deposition.

**Acknowledgment.** The valuable comments of the reviewers are gratefully acknowledged. This work was supported by the Department of Science and Technology, Government of India.

## References and Notes

(1) Kolb, D. M.; Prazasnyski, M.; Gerischer, H. *J. Electroanal. Chem.* **1974**, *54*, 25.

(2) Kolb, D. M. In *Advances in Electrochemistry and Electrochemical Engineering*; Gerischer, H., Tobias, C. W., Eds.; John Wiley-Interscience: New York, 1978; Vol. 11, p 125.

(3) Holze, R. *J. Solid State Electrochem.* **1998**, *2*, 73.

(4) Gichuhi, A.; Shannon, C. *Langmuir* **1999**, *15*, 5654.

(5) Chen, C.; Kepler, K. D.; Gewirth, A. A.; Ocko, B. M.; Wang, J. *J. Phys. Chem.* **1993**, *97*, 7290.

(6) Li, J.; Abruna, H. D. *J. Phys. Chem. B* **1997**, *101*, 244.

(7) Jennings, G. K.; Laibinis, P. E. *J. Am. Chem. Soc.* **1997**, *119*, 5208.

(8) Ross, P. N. In *Structure of Electrified Interfaces*; Lipkowski, J., Ross, P. N., Eds.; VCH Publishers: New York, 1993.

(9) Leiva, E. *Electrochim. Acta* **1996**, *41*, 2185 and references therein.

(10) Rikvold, P. A.; Zhang, J.; Sung, Y. E.; Wieckowski, A. *Electrochim. Acta* **1996**, *41*, 2175.

(11) Sudha, V.; Sangaranarayanan, M. V. *J. Phys. Chem. B* **2002**, *106*, 2699.

(12) Under electronic equilibrium, $\Delta\Phi$ equals $\Delta\Psi$ since the Fermi levels of the metal and the solution are identical. See for example: Schmickler, W. *Interfacial Electrochemistry*; Oxford University Press: London, 1996; Chapter 2.

(13) Fried, I.; Barak, H. *J. Electroanal. Chem.* **1971**, *30*, 279.

(14) Angerstein-Kozlowska, H.; Macdougall, B.; Conway, B. E. *J. Electroanal. Chem.* **1972**, *39*, 287.

(15) Gu, R. A.; Cao, P. G.; Sun, Y. H.; Tian, Z. Q. *J. Electroanal. Chem.* **2002**, *528*, 121.

(16) Yamashita, K.; Imai, H. *Bull. Chem. Soc. Jpn.* **1977**, *50*, 1066.

(17) Daum, W.; Dederichs, F.; Muller, J. E. *Phys. Rev. Lett.* **1998**, *80*, 766.

(18) Pemberton, J. E. In *Electrochemical Interfaces: Modern Techniques for in-situ interface characterization*; Abruna, H. D., Ed.; VCH Publishers Inc: New York, 1991; Chapter 5.

(19) Coetzee, J. F.; Campion, J. J. *J. Am. Chem. Soc.* **1967**, *89*, 2517.

(20) White, J. H.; Abruna, H. D. *J. Electroanal. Chem.* **1991**, *300*, 521.

(21) *CRC Hand Book of Chemistry and Physics*, 80th ed.; Lide, D. R., Ed.; CRC Press Inc.: Boca Raton, FL, 2000.

(22) Pauling, L. *The Nature of Chemical Bond*, 3rd ed.; Cornell University Press: Ithaca, NY, 1960; Chapters 3 and 11.

(23) Aurbach, D.; Daroux, M. L.; Faguy, P. W.; Yeager, E. *J. Electrochem. Soc.* **1987**, *134*, 1611.

(24) Aurbach, D.; Gottlieb, H. *Electrochim. Acta*, **1989**, *34*, 141.

(25) Goren, E.; Chusid, O.; Aurbach, D. *J. Electrochem. Soc.* **1991**, *138*, L6.

(26) Gregory, B. W.; Norton, M. L.; Stickney, J. L. *J. Electroanal. Chem.* **1990**, *293*, 85.

(27) Xing, X.-K.; Abel, P.; McIntyre, R.; Scherson, D. *J. Electroanal. Chem.* **1987**, *216*, 261.

(28) Ozoemena, K.; Nyokong, T. *Electrochim. Acta* **2002**, *47*, 4035.

(29) See for example: Conway, B. E.; Gileadi, E.; Dzieciuch, M. *Electrochim. Acta* **1963**, *8*, 143.

(30) See for example: Noel, M.; Vasu, K. I. *Cyclic Voltammetry and the Frontiers of Electrochemistry*; Aspect Publishers: London, 1990; Chapter 7.

(31) Hills, G. J.; Schiffrin, D. J.; Thompson, J. *J. Electrochem. Soc.* **1973**, *120*, 157.

(32) For the system Au/$Li^+$(ACN), numerical integration of the cyclic voltammetric peak yields $q_p$ ca. 680 $\mu$C $cm^{-2}$.

(33) James, S. D. *J. Electrochem. Soc.* **1975**, *122*, 921.

(34) Hansen, M.; Anderko, K. *Constitution of Binary Alloys*; McGraw-Hill Inc.: New York, 1958.

(35) Dey, A. N. *J. Electrochem. Soc.* **1971**, *118*, 1547.

(36) Romeo, F. M.; Tucceri, R. I.; Posadas, D. *Surface Sci.* **1988**, *203*, 186.

(37) Adzic, R; Yeager, E; Cahan, B. D. *J. Electrochem Soc.* **1974**, *121*, 474.

(38) Vaskevich, A.; Rubinstein, I. *J. Electroanal. Chem.* **2000**, *491*, 87.

(39) See for example: Parr, R. G.; Yang, W. *Density Functional theory of atoms and molecules*; Oxford University Press: New York, 1989.

(40) Trasatti, S. In *Advances in Electrochemistry and Electrochemical Engineering*; Gerischer, H., Tobias, C. W., Eds.; John Wiley-Interscience: New York, 1978; Vol. 10.

(41) Jasinski, R. In *Advances in Electrochemistry and Electrochemical Engineering*; Gerischer, H., Tobias, C. W., Eds.; John Wiley-Interscience: New York, 1978; Vol. 8, p 253.

(42) Bockris, J. O'M.; Conway, B. E. *Modern Aspects of Electrochemistry*; Butterworth Scientific Publications: London, 1954; Vol. 1, Chapter 2, p 71.

(43) Padova, J. I. In *Modern Aspects of Electrochemistry*; Conway, B. E., Bockris, J. O'M., Eds.; Butterworths: London, 1972; Vol. 7, Chapter 1.

(44) Hamann, C. H.; Hamnett, A.; Vielstich, W. *Electrochemistry*; Wiley-VCH Publishers: New York, 1998; Chapter 9.

(45) Conway, B. E. *Electrochemical Supercapacitors: Scientific Fundamentals and Technological Applications*; Kluwer Academic/Plenum Publishers: New York, 1999; Chapter 10.

(46) Schnidler, W.; Hofmann, D.; Kirschner, J. *J. Appl. Phys.* **2000**, *87*, 7007.

(47) Huckaby, D. A.; Blum, L. *J. Chem. Phys.* **1990**, *92*, 2646.

(48) Huckaby, D. A.; Blum, L. *J. Electroanal. Chem.* **1991**, *315*, 255.

(49) Huckaby, D. A.; Blum, L. In *Diffusion processes: Experiment, Theory, Simulations*; Proceedings of the 5th Max Born Symposium, Kudowa, Poland, June 1994; Pekalski, A., Ed.; Springer-Verlag: Berlin, 1994.

(50) Garland, J. E.; Assiongbon, K. A.; Pettit, C. M.; Emery, S. B.; Roy, D. *Electrochim. Acta* **2002**, *47*, 4113.

(51) For the systems Pt/$Li^+$, Pt/$Na^+$, and Pt/$Cs^+$ in PC, $i_p$ is obtained by dividing the peak current by the area of the electrode (0.12 $cm^2$). The peak currents of the above-mentioned systems are evaluated as ca. 13.4, 6.4, and 2.0 $\mu$A, respectively, from their corresponding stripping voltammetry (cf. ref 13).

(52) The experimental $E_{ML}$ and $E_B$ values have been reported with reference to the saturated calomel electrode (SCE), and hence, $E°$ ($Li^+$/Li) is also converted accordingly.

(53) (a) Yeager, H. L.; Fedyk, J. D.; Parker, R. J. *J. Phys. Chem.* **1973**, *77*, 2407. (b) The solvation number of $Cu^+$ in ACN has been assumed to be eight.

(54) Bockris, J. O'M.; Conway, B. E. *Modern Aspects of Electrochemistry*; Butterworth Scientific Publications: London, 1954; Vol 1, Chapter 2, p 64.